Electronic Supplementary Material (ESI) for Energy & Environmental Science.

Supporting Information

A Schiff Base Modified Gold Catalyst for Green and Efficient H_2 Production from Formic Acid

Qinggang Liu,[a,b] Xiaofeng Yang,[a] Yanqiang Huang,*[a] Shutao Xu,[a] Xiong Su,[a] Xiaoli Pan,[a] Jinming Xu,[a] Aiqin Wang,[a] Changhai Liang,[b] Xinkui Wang*[b] and Tao Zhang*[a]

Experimental

1. Catalyst Syntheses

1.1 Preparation of Schiff base modified SiO_2 support.

The SiO_2 powders were prepared by the aldimine condensation of (3-aminopropyl) triethoxysilane (APTES) with formaldehyde. Typically, 10 mL HCHO solution (37%) was added into 0.134 mol L^{-1} APTES aqueous solutions while stirring at 30 °C (HCHO/APTES, mol/mol = 5.0). The resulting white precipitation generated by aldimine condensation was then filtered and washed with deionized water and dried under reduced pressure to obtain Schiff base-functionalized SiO_2 support.

1.2 Preparation of Au@Schiff-SiO_2 catalyst.

Gold NPs with encapsulating structure were prepared by *in situ* reduction method. Briefly, 1.0 g Schiff base-functionalized SiO_2 was impregnated with an aqueous solution of $HAuCl_4$ (0.5 mM, 150 mL), after reflux for 2 h at 100 ^{o}C under stirring, the mixture was transferred into a Teflon-lined autoclave and maintained at 105 °C for 12 h (*Au NPs will trapped into the metastable SiO_2 support due to the condensation of silicon hydroxyl groups in hydrothermal process*). After the autoclave was cooled down to room temperature naturally, the precipitate was filtered and washed with an excess amount of deionized water until no chlorine ions were detected in the filtrate. Following drying in vacuum at 120 ^{o}C for 12 h, Au@Schiff–SiO_2 catalyst was obtained.

1.3 Preparation of Au/SiO_2-Schiff Catalyst.

Gold NPs supported on the surface of Schiff base-functionalized SiO_2 were prepared by a sodium borohydride reduction method. First, the abovementioned metastable SiO_2 was transferred into a Teflon-lined autoclave and maintained at 150 °C for 12 h to enhance its stability, followed by drying at 120 ^{o}C for 12 h. Subsequently, 1.0 g of the obtained stable SiO_2 was impregnated with an aqueous solution of $HAuCl_4$ (1.01 mM, 150 mL), the resulted aqueous suspension was further homogenized under stirring for half an hour. Then, 15 mL of 0.2 M $NaBH_4$ solution was added into the above obtained solution with vigorous stirring, the mixture was stirred for another half an hour at room temperature to fully deposit the metallic nanoparticles onto the support. Finally, the desired catalyst Au/SiO_2-Schiff was collected by filtering and washed with an excess amount of deionized water until no chlorine ions were detected in the filtrate, following drying in vacuum at 120 ^{o}C for 12 h.

1.4 Preparation of Au/SBA-15-NH_2 catalyst.

SBA-15 mesoporous silica was synthesized using P123 as templating agent in acidic solution, as reported previously by Zhao et al.[S1] Prior to the metal deposition, SBA-15 support was first functionalized with APTES ($H_2N(CH_2)_3$-$Si(OEt)_3$). Briefly, 1.0 g of SBA-15 was mixed and stirred with 2.1 mmol of APTES in 150 mL of anhydrous ethanol for 12 h at 80 °C to graft the mesoporous SBA-15 with primary amine groups. After filtration and washed with ethanol, "SBA-15-NH_2" was obtained by drying in vacuum at 120 ^{o}C for 12 h.

Au NPs supported on the surface of SBA-15-NH_2 were prepared by the same synthetic procedure as that for Au/SiO_2-Schiff catalyst, and the obtained catalyst was denoted as Au/SBA-15-NH_2.

1.5 Preparation of Pd@Schiff-SiO$_2$ Catalyst.

Pd@Schiff-SiO$_2$ catalyst was prepared by the same synthetic procedure as that for Au@Schiff – SiO$_2$ catalyst, wherein the precursor is PdCl$_2$ aqueous solution.

1.5 Preparation of unfunctionalized Au/SiO$_2$ and Au/SBA-15 Catalysts.

Firstly, the amine-functionalized Au/SiO$_2$ and Au/SBA-15 catalysts were prepared by the same synthetic procedure as described in **1.2** and **1.4** with a theory loading of 1.0 wt% and 1.5 wt%, respectively. The achieved amine-functionalized catalysts were then calcined at 500 °C for 4 h to obtain the pure Au/SiO$_2$ and Au/SBA-15 Catalysts.

2. Catalytic Activity Characterization

2.1 Procedure for the decomposition of formic acid:

The hydrogen production from FA solution was carried out in a 10 mL vessel at a preset temperature (25-50 °C) under ambient atmosphere. In general, 30 mg of catalyst was first placed in the vessel, then 3.3 mL FA solutions containing 5.0 mmol of FA was injected quickly. A gas burette filled with water was connected to the reaction vessel to measure the volume of released gas. The reforming gas composition was analysed by Agilent gas chromatograph (GC) with a TDX-01 column connected to a thermal conductivity detector (TCD).

2.2 Durability testing of Au @Schiff-SiO$_2$:

The catalyst reuse experiment was carried out in 10 M FA solution. Briefly, 0.75 mL of pure FA (20 mmol) was subsequently added into the reaction vessel after the completion of the first-run decomposition of FA. Such test cycles of the catalyst for the decomposition of FA were carried out for 5 runs at 50 °C by adding 0.75 mL pure FA.

3. Calculation of turnover frequency (TOF)

The initial TOF reported here is calculated by total amount of gas volume (H$_2$ + CO$_2$) at 5 min from the equation as follow:

$$TOF = \frac{P_0 V}{2 R T n_{Au} t}$$

where P$_0$ is the atmospheric pressure (101325 Pa), V is the generated volume of (H$_2$ + CO$_2$) gas, R is the universal gas constant (8.3145 m^3 Pa mol^{-1} K^{-1}), T is the room temperature (298 K), n$_{Au}$ is the total mole number of Au atoms in catalyst and *t* is the initial time of the catalytic reaction (5 min).

4. Catalyst characterization

4.1 Elemental analysis

The Au loading of the catalysts was measured by inductively coupled plasma atomic emission spectroscopy (ICP-AES) on an IRIS Intrepid II XSP instrument (Thermo Electron Corporation).

4.2 NMR

All the solid state NMR experiments were performed on a Bruker AvanceIII 600 spectrometer equipped with a 14.1 T wide-bore magnet. The resonance frequencies were 156.4 and 119.2 MHz for ^{13}C, and ^{29}Si, respectively. ^{1}H→^{13}C and ^{1}H→^{29}Si CP/MAS NMR experiments were performed on a 4 mm MAS probe with a spinning rate of 12 and 8 kHz, respectively. ^{1}H→^{13}C CP/MAS NMR experiments were carried out with a contact time of 5 ms and a recycle delay of 2 s. The chemical shifts were referenced to adamantane with the upfield methine peak at 29.5 ppm. $^{1}H \rightarrow ^{29}Si$ CP/MAS NMR experiments were carried out with a contact time of 3 ms and a recycle delay of 2 s. Chemical shifts were referenced to 4,4-dimethyl-4-silapentane sulfonate sodium salt (DSS).

4.3 High-angle annual dark-filed scanning transmission electron microscopy (HAADF-STEM)

HAADF-STEM images were obtained using a JEOL JEM-2100F at 200 kV. The samples for electron microscopy were prepared by grinding and subsequent dispersing the powder in ethanol and applying a drop of very dilute suspension on carbon-coated grids.

4.4 High resolution scanning electron microscopy (HR-SEM)

HR-SEM observations were carried out on a JSM 7800F scanning electron microscope (JEOL, Japan). ***Notice that both secondary electron (SE, emitted from the extreme surface) and backscattered electron (BSE, emitted from a greater depth) images were executed on the same area to reveal the Au NPs were trapped inside or exposed on the surface of the support.***

4.5 X-ray photoelectron spectroscopy (XPS)

XPS was performed on a Kratos AXIS ULTRA DLA X-ray photoelectron spectrometer equipped with an Al Kαradiation source (1486.6 eV, 15 kV). All binding energies were calibrated with the C1s peak at 284.8 eV for the adventitious carbon.

4.6 Fourier transform infrared (FTIR) spectroscopy

The FTIR spectra were acquired with a spectrometer (Bruker tensor27) equipped with a DLATGS detector and operated at a resolution of 4 cm^{-1}.

4.7 CHN elemental analysis

CHN elemental analysis was performed on Vario EL III (Elementar, Hanau, Germany). Elemental analysis result of Au@Schiff-SiO_2, Au/SiO_2-Schiff and Au/SBA-15-NH_2 was shown in Table S1.

Table S1. Elemental analysis result of Au@Schiff-SiO_2, Au/SiO_2-Schiff and Au/SBA-15-NH_2 catalysts.

Entry	Catalyst	Carbon (wt%)	Hydrogen (wt%)	Nitrogen (wt%)
1	Au/SBA-15-NH_2	5.1	1. 5	1.1
2	Au/SiO_2-Schiff	33.7	5.7	7.6
3	Au@Schiff-SiO_2	33.5	5.9	7.9

Table S2. Metal loadings and surface atomic ratios of the prepared catalysts.

Catalyst	Metal loading [a] (wt%)	atomic ratios (%)[b]		
		C	Au	N
Au/SBA-15-NH_2	1.0	14.7	0.08	1.5
Au/SiO_2-Schiff	2.6	51.8	0.76	8.2
Au@Schiff-SiO_2	3.2	53.2	0.48	8.8
Au/SBA-15	2.4	2.9	0.04	0.24
Au/SiO_2	2.8	4.8	0.17	0.48

[a] The actual metal loading was measured by ICP-AES.

[b] The atomic ratios were measured by XPS.

Table S3. Catalytic activities for dehydrogenation of formic acid catalyzed by recently reported heterogeneous catalysts.

Catalyst	Temp. /°C	Additives	FA / M	TOF /h^{-1}	Ref.
Au@Schiff-SiO_2	**50**	**none**	**10**	**4368**	**This work**
Au@Schiff-SiO_2	**50**	**none**	**pure**	**2882**	**This work**
SBA-15-NH_2 /Pd	26	none	1.0	377	[S2]
$Ag_{42}Pd_{58}$	50	none	1.0	382	[S3]
$Co_{0.3}Au_{0.35}Pd_{0.35}$	25	none	0.5	80	[S4]
Pd/mpg-C_3N_4	25	none	1.0	144	[S5]
CrAuPd/N-SiO_2	25	none	0.2	730	[S6]
Au/ZrO_2 NCs	50	NEt_3	10.6	1593	[S7]
Au@SiO_2_AP	90	HCOONa	3.0	400 [a]	[S8]
Pd/MSC-30	50	HCOONa	6.0	2623	[S9]
AuPd@ED-MIL-101	90	HCOONa	3.0	106	[S10]
Pd-B/C	30	HCOONa	1.1	1184	[S11]
$Ag_{0.1}Pd_{0.9}$/RGO	50	HCOONa	0.7	2739	[S12]
Ir-DHBP [b]	**60**	**none**	**pure**	**760**	**[S13]**

[a] TOF values were calculated according to the amount of released H_2 in overall testing time.

[b] DHBP= 4,4'-dihydroxy-2,2'-bipyridine.

References

[S1] D. Zhao, J. Feng, Q. Huo, N. Melosh, G. H. Fredrickson, B. F. Chmelka, G. D. Stucky, Science, 1998, 279, 548-552.

[S2] K. Koh, J. E. Seo, J. H. Lee, A. Goswami, C.W. Yoon, T. Asefa, J. Mater. Chem. A, 2014, 2, 20444-20449

[S3] S. Zhang, Ö. Metin, D. Su, S. Sun, Angew. Chem. Int. Ed., 2013, 52, 3681-3684

[S4] Z. L. Wang, J. M. Yan, Y. Ping, H. L. Wang, W. T. Zheng, Q. Jiang, Angew. Chem. Int. Ed., 2013, 52, 4406-4409.

[S5] J. H. Lee, J. Ryu, J. Y. Kim, S.-W. Nam, J. H. Han, T.-H. Lim, S. Gautam, K. H. Chae, C. W. Yoon, J. Mater. Chem. A, 2014, 2, 9490-9495.

[S6] M. Yurderi, A. Bulut, N. Caner, M. Celebi, M. Kaya, M. Zahmakiran, Chem. Commun., 2015, 51, 11417-11420.

[S7] Q. Y. Bi, X. L. Du, Y. M. Liu, Y. Cao, H. Y. He, K. N. Fan, J. Am. Chem. Soc., 2012, 134, 8926-8933.

[S8] M. Yadav, T. Akita, N. Tsumori, Q. Xu, J. Mater. Chem., 2012, 22, 12582-12586.

[S9] Q. L. Zhu, N. Tsumori, Q. Xu, Chem. Sci., 2014, 5, 195-199.

[S10] X. Gu, Z. H. Lu, H. L. Jiang, T. Akita, Q. Xu, J. Am. Chem. Soc., 2011, 133, 11822-11825.

[S11] K. Jiang, K. Xu, S. H. Zou, W. B. Cai, J. Am. Chem. Soc., 2014, 136, 4861-4864.

[S12] Y. Chen, Q. L.Zhu, N. Tsumori, Q. Xu, J. Am. Chem. Soc., 2015, 137, 106-109.

[S13] Y. Himeda, Green Chem., 2009, 11, 2018-2022.

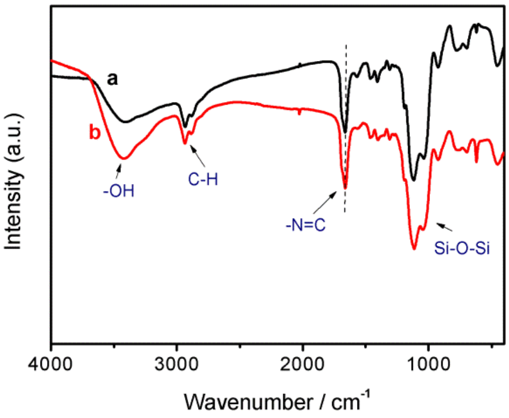

Fig. S1 FT-IR spectra of Au@Schiff-SiO_2 before (a) and after (b) catalytic decomposition of FA.

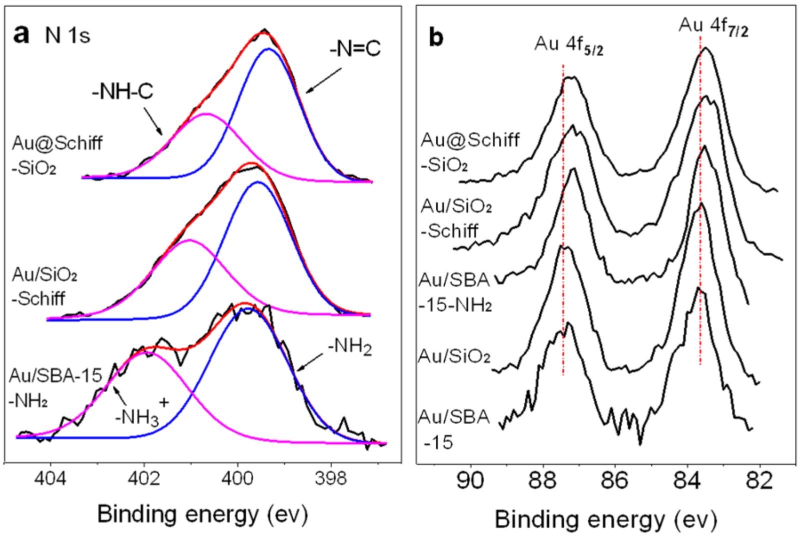

Fig. S2 Core level XPS spectra in Au 4f (a) and N 1s (b) regions of as-prepared Au@Schiff-SiO_2, Au/SiO_2-Schiff, Au/SBA-15-NH_2, Au/SiO_2 and Au/SBA-15.

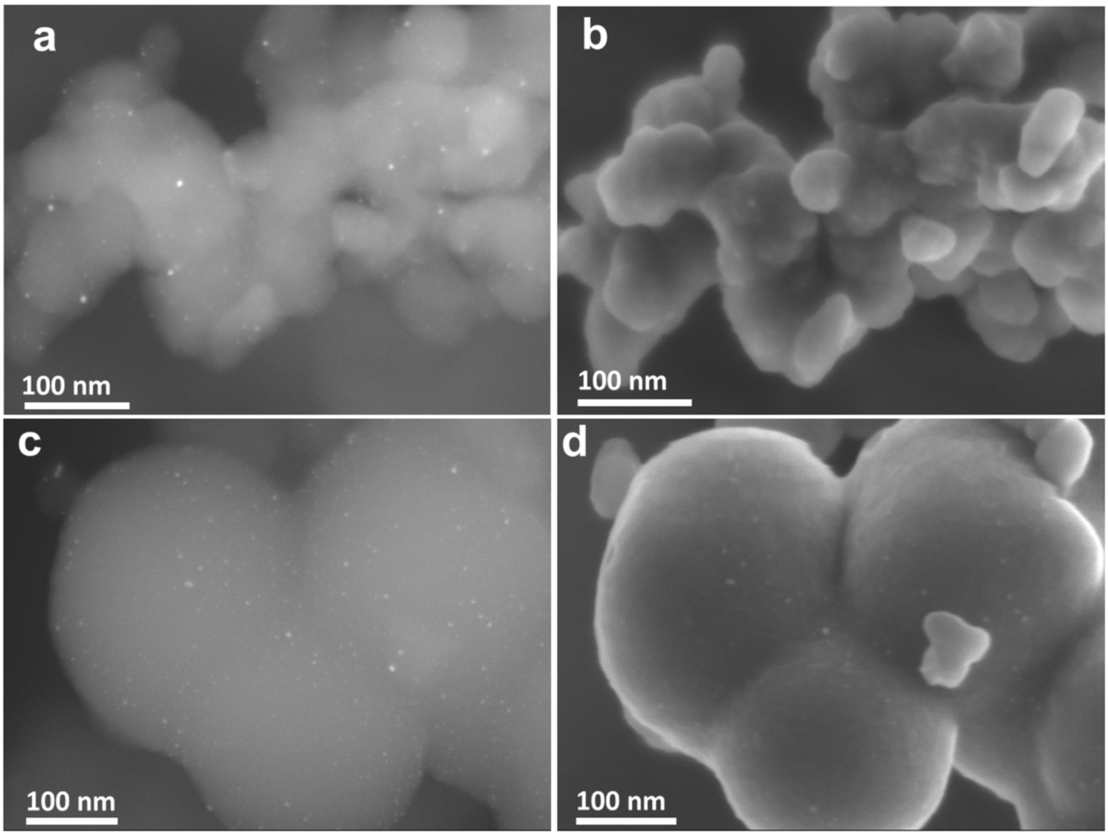

Fig. S3 HR-SEM images of Au@Schiff-SiO_2 (up) and Au/SiO_2-Schiff (down), where (a) and (c) were BSE image, (b) and (d) were SE image. The bright spots are Au particles.

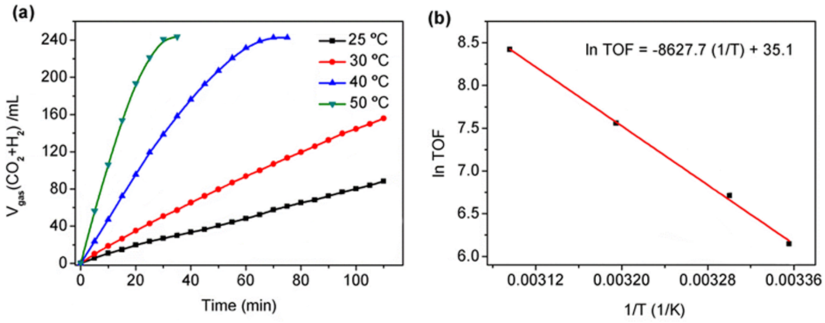

Fig. S4 (a) The volume of CO_2 +H_2 generated vs. time for the catalytic FA dehydrogenation at different temperatures and (b) the related Arrhenius plot (lnTOF vs. 1/T). Reaction conditions: 5.0 mmol FA (1.5 M), 30 mg Au@Schiff-SiO_2, 50 ^{o}C.

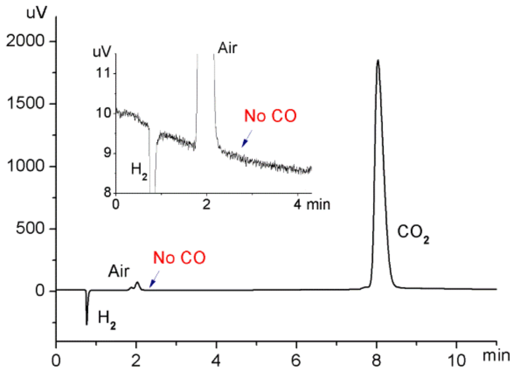

Fig. S5 Gas chromatogram of the evolved gas from FA aqueous solution over Au@Schiff-SiO$_2$ at 50 ^{o}C. The absence of CO signal at about 2.5 min suggests that the CO content is below the instrumental detection limit of 2 ppm.

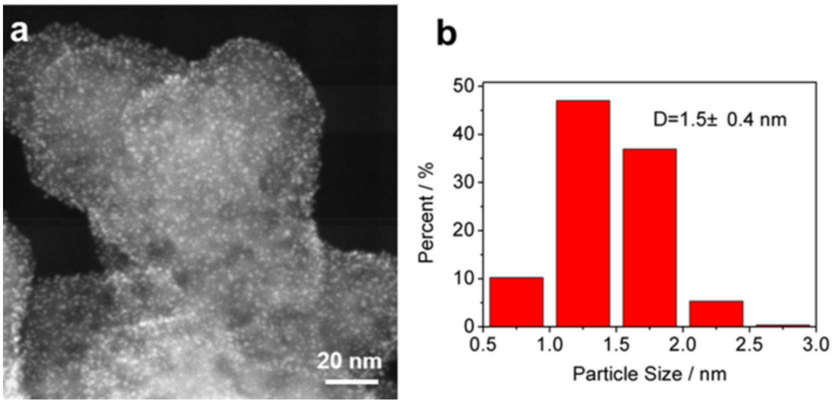

Fig. S6 HAADF-STEM image of Pd@Schiff-SiO$_2$ (a) and the corresponding particle size distribution histograms (b).

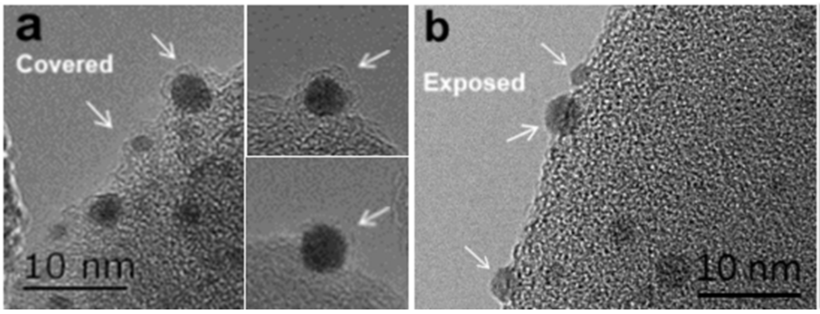

Fig. S7 HR-TEM images of (a) Au@Schiff-SiO$_2$ and (b) Au/SiO$_2$-Schiff.

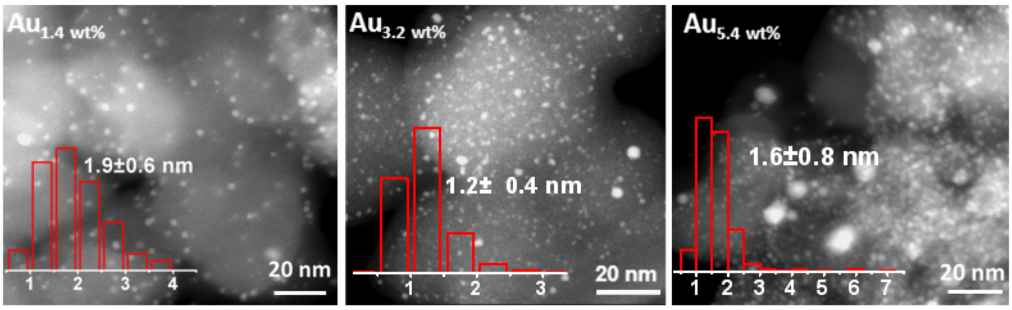

Fig. S8. HAADF-STEM images of the prepared Au$_{1.4wt\%}$@Schiff-SiO$_2$, Au$_{3.2wt\%}$@Schiff-SiO$_2$ and Au$_{5.4wt\%}$@Schiff-SiO$_2$.

As shown in Fig. S8, with lower loadings, ~2 nm gold nanoparticles were highly dispersed on the catalyst surface without any aggregation. Though aggregation was induced by the increase of gold loadings, much more smaller gold nanoparticles were formed with a diameter of <1.5 nm both for Au$_{3.2\ wt\%}$/SiO$_2$-Schiff and Au$_{5.4\ wt\%}$/SiO$_2$-Schiff, which was only a little proportion over Au$_{1.4\ wt\%}$/SiO$_2$-Schiff.

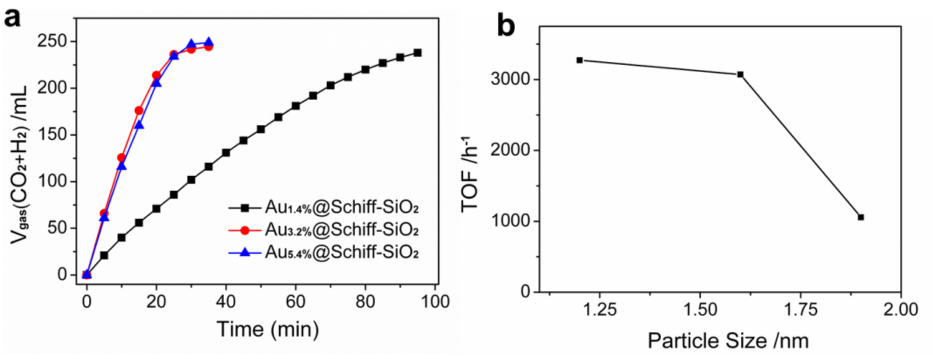

Fig. S9. Schiff base functionalized gold catalysts for formic acid dehydrogenation with different loadings. Reaction conditions: 4.8 µmol metal, 50 °C, 5 mmol formic acid (1.5 M).

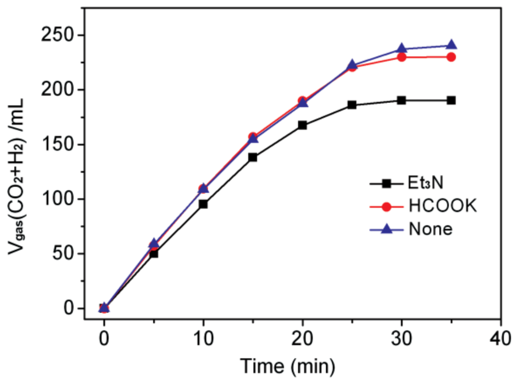

Fig. S10 The effects of base and formate on the FA dehydrogenation over Au@Schiff-SiO$_2$ catalyst

Reaction conditions: 5.0 mmol FA (1.5 M), 30 mg catalyst, 1 mmol additives, 50 °C.

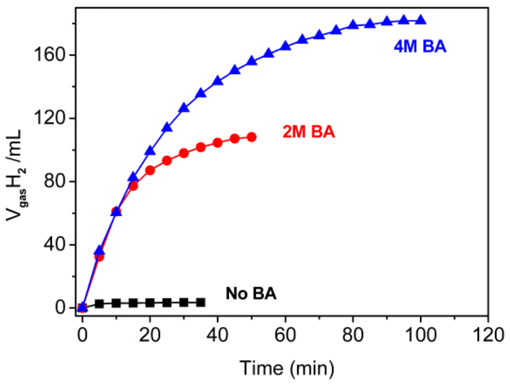

Fig. S11 Decomposition of potassium formate catalyzed by Au@Schiff-SiO$_2$ with or without boric acid (BA).

Reaction conditions: 7.5 mmol PF (1.5 M), 80 °C, 30 mg catalyst.

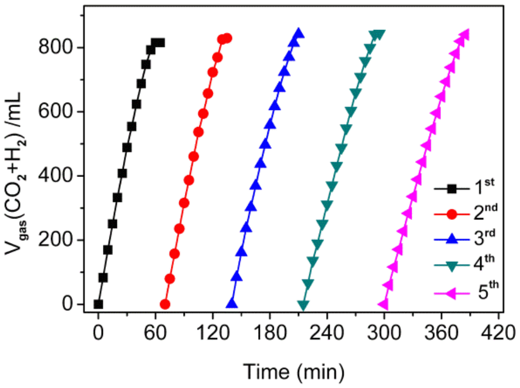

Fig. S12 Reuse of the Au@Schiff-SiO_2 catalyst for the catalytic FA dehydrogenation. Reaction conditions: 20 mmol FA (10 M), 30 mg catalyst, 50 °C.

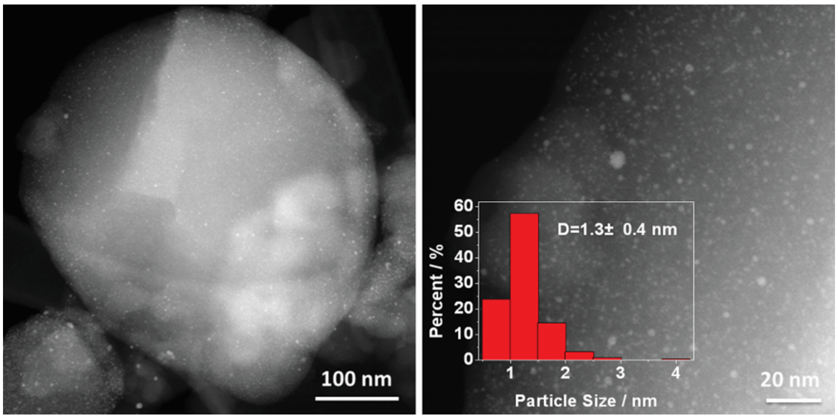

Fig. S13 HAADF-STEM images of Au@Schiff-SiO_2 after catalytic decomposition of FA.

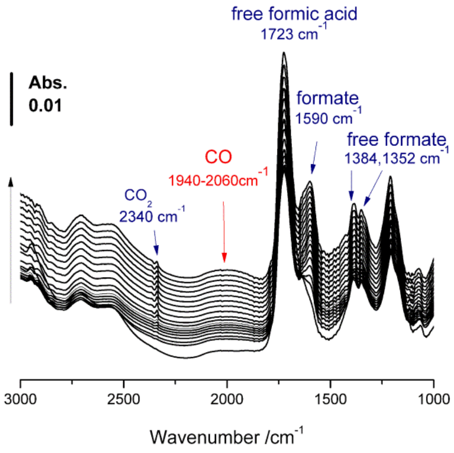

Fig. S14. Time-evolved *in situ* FT-IR spectra of Pd@Schiff-SiO$_2$ recorded after injecting 1 μL pure FA to the sample sheet. Reference spectrum was recorded in air before the injection, and the acquisition time for each single-beam spectrum is 40 s.